Local dynamics of *cis*-polyisoprene in dilute solution and in the melt: a fluorescence anisotropy decay study

Valérie Veissier, Jean-Louis Viovy* and Lucien Monnerie
Laboratoire PCSM, ESPCI, 10 rue Vauquelin, F75231 Paris Cedex 05, France
(Received 6 December 1988; accepted 6 January 1989)

The local dynamics of a polyisoprene labelled with anthracene in the middle of the chain are investigated both in decalin solution and in bulk polyisoprene using the fluorescence anisotropy decay technique. Several types of orientational autocorrelation functions have been tested. Hall and Helfand's expression accounts for the experimental data in the case of solution, whereas the generalized diffusion and loss model is more satisfactory in the case of bulk polymer. The influence of various parameters (such as temperature, medium and nature of the polymer chain) on correlation times is discussed. It is shown that the orientational memory is stronger in the bulk than in a solvent of small molecules.

(Keywords: polyisoprene; fluorescence anisotropy decay; local dynamics; bulk polymer; dilute solution; correlation time; orientational autocorrelation function)

INTRODUCTION

Among the different questions of interest for polymer dynamics, local motions are still poorly understood. Because of the number of degrees of freedom of polymer chains, they generally exhibit a non-exponential time orientational autocorrelation function (OACF). Numerous shapes were suggested for the OACF during the past[1–9]. Several experiments using polymer solutions have been carried out during the last decade. Polystyrene[7,10], polyisoprene[11] and poly(methyl methacrylate)[12] have been studied in different solvents. Fewer experiments have been performed on bulk polymers. The dynamics of bulk polybutadiene were recently investigated by Viovy *et al.*[6]. Unfortunately, these experiments are not directly comparable. The aim of this paper is to investigate and to compare the local dynamics of the same polymer in bulk as well as in solution. The dynamics of a polyisoprene with a high *cis* content (IR307) is studied using the fluorescence anisotropy decay (FAD) technique. This method is a powerful one for investigating local dynamics since it provides continuous sampling of the orientational autocorrelation function. In the next section, the models of motion available are reviewed. The experimental method is then described. The results, which were briefly reported in ref. 13, are given in detail and interpreted, and conclusions are proposed in the final section.

ORIENTATIONAL AUTOCORRELATION FUNCTIONS OF POLYMERS

Rotational diffusion models[14–16] do not take into account the flexible nature of polymer chains, and indeed they fail to describe the autocorrelation function of polymers in a consistent way[5,6,10,17]. The linear structure of usual macromolecules correlates the motions of individual bonds (conformational jumps) along the main chain. Several methods based on a diffusion equation have been suggested during the past to express the orientational autocorrelation function (OACF)[1–4]. They have been extensively discussed in previous papers[5,6]. The correlation leads to a non-exponential term in the OACF, related to a characteristic time τ_1. The OACF usually also includes an exponential term with characteristic time τ_2, which describes the damping of the main-chain motion (see e.g. expressions VJGM, BY and JS in *Table 1*).

Another approach is found in Hall and Helfand's work[7]. These authors calculated a conformational autocorrelation function (CACF) for a chain of two-state elements[7]:

$$C(t)=\exp(-t/\tau_1)\exp(-t/\tau_2)I_0(t/\tau_1) \qquad (1)$$

Using computer simulations, Weber and Helfand[8] showed that the expression for the CACF can be used to describe the OACF. Indeed, this is not very surprising, since the mathematical solution of the HH model presents strong similarities with that of the one-dimensional diffusion equation. Viovy *et al.*[5] generalized this expression on an empirical basis:

$$C(t)=\exp(-t/\tau_1)\exp(-t/\tau_2)\left[I_0(t/\tau_1)+\sum_{q=1}^{N} a_q I_q(t/\tau_1)\right] \qquad (2a)$$

in which N is the number of bonds. This expression is generally restricted to the first order $q=1$ and $a_q=1$:

$$C(t)=\exp(-t/\tau_1)\exp(-t/\tau_2)[I_0(t/\tau_2)+I_1(t/\tau_1)] \qquad (2b)$$

More recently, Lin *et al.*[9] extended Jones and Stockmayer's model[3] within the continuous limit, and put this extension on a firm theoretical ground:

$$C(t)=\exp(-t/\tau_1)\left[I_0(t/\tau_1)+2\sum_{q=1}^{N}\exp(\gamma q)+I_q(t/\tau_1)\right] \qquad (3)$$

* To whom correspondence should be addressed

0032-3861/89/071262-07$03.00

Table 1 Expressions for the OACF tested in the present paper

Reference	Abbreviation	Autocorrelation function
Williams and Watts[18]	WW	$\exp[(-t/\tau_1)^{\beta}]$
Valeur *et al.*[1,2]	VJGM	$\exp(-t/\theta)\exp(t/\rho)\,\mathrm{erfc}[(t/\rho)^{1/2}]$
Jones and Stockmayer[3]	JS_n	$\sum_{k=1}^{n} a_k \exp(-t/\tau_k)$
Bendler and Yaris[4]	BY	$\frac{1}{2}(\pi/t)^{1/2}(1/\sqrt{\tau_1}-1/\sqrt{\tau_2})[\mathrm{erfc}(t/\tau_2)^{1/2}-\mathrm{erfc}(t/\tau_1)^{1/2}]$
Hall and Helfand[7]	HH	$\exp(-t/\tau_2)\exp(-t/\tau_1)I_0(t/\tau_1)$
Lin *et al.*[9]	LJS	$\exp(-t/\tau_1)[I_0(t/\tau_1)+aI_1(t/\tau_1)]$
Viovy *et al.*[5]	GDL	$\exp(-t/\tau_2)\exp(-t/\tau_1)[I_0(t/\tau_1)+I_1(t/\tau_1)]$
Generalization[9]	LJS*	$\exp(-t/\tau_2)\exp(-t/\tau_1)[I_0(t/\tau_1)+aI_1(t/\tau_1)]$

where γ is equal to 2 ln 3 for a tetrahedral lattice. In this expression, diffusion along the main chain is taken into account but the damping effect is not. Including this effect, formula (3) may be generalized as:

$$C(t)=\exp(-t/\tau_2)\exp(-t/\tau_1)\times\left[I_0(t/\tau_1)+2\sum_{q=1}^{N}\exp(\gamma q)I_q(t/\tau_1)\right] \quad (4a)$$

or, considering first order only:

$$C(t)=\exp(-t/\tau_2)\exp(-t/\tau_1)[I_0(t/\tau_1)+aI_1(t/\tau_1)] \quad (4b)$$

The expressions for the OACF tested in the present paper are summarized in *Table 1*.

EXPERIMENTAL

The fluorescence anisotropy decay technique has been fully described in refs. 5 and 6. Therefore, we restrict this section to a short review of the principle of the experiment. A polymer is labelled with a fluorescent probe in the middle of the chain. The transition moment of the probe lays along the local axis of the backbone of the macromolecule. A vertically polarized nanosecond pulse provided by a synchrotron source excites the fluorophore. Parallel and perpendicular components of the fluorescence I_v and I_h are recorded as a function of time t. The time-dependent anisotropy $r(t)$ is evaluated using:

$$r(t)=\frac{I_v(t)-I_h(t)}{I_v(t)+2I_h(t)}=r_0C(t) \quad (5)$$

$r(t)$ is proportional to the autocorrelation function $C(t)$ and to the fundamental anisotropy r_0, which is independent of t.

The experiments were performed on the A3 beam line of the cyclosynchrotron LURE-ACO (Orsay, France) (the fluorescence anisotropy equipment has been described elsewhere[5,6,10]). The data were analysed at the CNRS-Circe computing centre by means of an iterative reconvolution algorithm[5,10]. Several criteria were used to discuss curve fitting. The fit is accepted when:

(a) χ^2 approaches 1 (χ^2 equals 1 for purely statistical deviations and increases concomitantly with non-random deviations); generally speaking, the comparison of χ^2 for different fits to the same data sets leads us to choose the model whose χ^2 is the closest to 1.

(b) The distribution of weighted residuals is random.

(c) r_0 does not exceed 0.4.

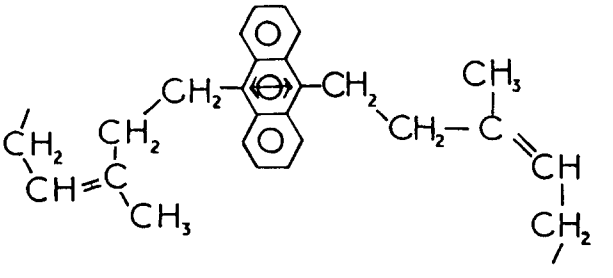

Figure 1 Polyisoprene labelled with anthracene (PIAPI) (the double arrow represents the transition moment)

(d) The values of the fitted parameters are stable for different truncations of the data set; the truncations used in the present paper are the following:

(1) 0 to 75 ns
(2) 0 to 57 ns
(3) 0 to 24 ns for bulk polymer
(4) 3.2 to 57 ns
(5) 6.4 to 57 ns

0.86 to 20 ns for polymer solution

As shown by Wahl[11,12], the best truncation depends on the lifetime of the probe ϕ and its correlation time τ. In the case of a monoexponential fluorescence and a monoexponential anisotropy decay, the optical experimental window is given by:

$$\Delta t=5\tau\phi/(2\phi+\tau)$$

The anthracene-labelled polyisoprene (*Figure 1*), generously provided by La Manufacture des Pneumatiques Michelin, was obtained by deactivation of 'living' anionic polyisoprene using 9,10-bisbromomethylanthracene; its dynamics were studied both in bulk polyisoprene (IR307, provided by Shell) and in decalin solution (Prolabo). The polymers were purified by Soxhlet continuous extraction in acetone. Decalin was distilled under reduced pressure shortly before use. The characteristics of IR307 and labelled polyisoprene (PIAPI) are summarized in *Table 2*.

The optical density of the sample was set to 0.08 for a 10 mm optical path to avoid energy transfer as well as reabsorption. In the case of bulk polymer, a film 1 mm thick was moulded into a cell composed of two asymmetric quartz prisms as described in ref. 6. The experiments in decalin solution were performed using quartz cells with a 10 mm optical path.

Table 2 Characteristics of the polyisoprenes used in the present study

Sample	Nature	Symbol	T_g (K)	T_∞ (K)	M_n	Microstructure (%)		
						cis	*trans*	1–2
Polyisoprene	Unlabelled	IR307	211	146	182000	92	5	3
Polyisoprene	Labelled	PIAPI	211	146	480000	81	11	8
PI (Hyde *et al.*[16])					10800	39	36	25

Table 3 Best-fit parameters for the WW, VJGM and BY models at $T=332.7$ K (59.7°C) in melt PI

Model	Truncation	χ^2	r_0	τ_1 (ns)	τ_2 (ns)	τ_2/τ_1 (or β)
WW	(1)	1.2326	0.268	11.4		$\beta=0.736$
	(2)	1.2772	0.268	11.4		$\beta=0.732$
	(3)	1.5477	0.266	11.4		$\beta=0.757$
	(4)	1.2687	0.269	11.4		$\beta=0.731$
	(5)	1.2297	0.268	11.5		$\beta=0.733$
VJGM	(1)	1.3026	0.278	43.0	21.5	0.500
	(2)	1.3822	0.279	41.6	21.8	0.524
	(3)	1.6994	0.273	68.5	18.1	0.264
	(4)	1.3720	0.279	41.3	21.8	0.528
	(5)	1.3353	0.279	40.6	22.0	0.542
BY	(1)	1.3191	0.255	3.84	77.2	20.1
	(2)	1.3543	0.255	3.77	81.4	21.6
	(3)	1.4822	0.259	2.94	307	104
	(4)	1.3418	0.255	3.74	83.9	22.4
	(5)	1.2735	0.255	3.79	82.1	21.7

Table 4 Best-fit parameters for the JS model at $T=332.7$ K (59.7°C) in melt PI

Model	Truncation	χ^2	r_0	τ_1 (ns)
JS_1 (one bond)	(1)	2.9617	0.251	12.2
	(2)	3.6000	0.251	12.2
	(3)	4.0102	0.259	10.7
	(4)	3.7547	0.251	12.2
	(5)	3.6358	0.259	12.4
JS_3 (five bonds)	(1)	1.2383	0.267	13.3
	(2)	1.2709	0.267	13.3
	(3)	1.2564	0.264	13.9
	(4)	1.2863	0.267	13.3
	(5)	1.2662	0.267	13.3
JS_4 (seven bonds)	(1)	2.3137	0.272	11.9
	(2)	2.5553	0.272	12.0
	(3)	1.2738	0.266	13.4
	(4)	2.6503	0.272	12.0
	(5)	2.7317	0.272	12.0
JS_5 (nine bonds)	(1)	2.7045	0.272	11.9
	(2)	2.9689	0.272	12.0
	(3)	1.2764	0.267	13.3
	(4)	3.0897	0.272	12.0
	(5)	3.2005	0.271	12.0

STUDY OF BULK POLYISOPRENE

The dynamics of labelled polyisoprene in IR307 were investigated within the temperature range 293–363 K, in a nitrogen atmosphere. The comparison of models of motion is realized at two temperatures, 332.7 K (59.7°C) and 364.6 K (91.6°C), for which the OACF is well sampled in the experimental window. The best-fit parameters (for the different models) are gathered in *Tables 3–8*. *Figures 2–6* illustrate the difference between models at 59.7°C for truncation (1).

Table 5 Best-fit parameters for the HH, GDL and LJS models at $T=332.7$ K (59.7°C) in melt PI

Model	Truncation	χ^2	r_0	τ_1 (ns)	τ_2 (ns)	τ_2/τ_1
HH	(1)	1.3212	0.254	11.0	59	5.42
	(2)	1.3513	0.254	10.8	65	6.03
	(3)	2.0345	0.199	20.9	61	2.95
	(4)	1.3574	0.254	10.8	65	6.03
	(5)	1.3205	0.254	10.9	63	5.79
GDL	(1)	1.2053	0.257	5.42	37	6.95
	(2)	1.2214	0.257	5.32	38	7.29
	(3)	1.2589	0.260	4.34	61	14.2
	(4)	1.2339	0.257	5.31	38	7.30
	(5)	1.1963	0.257	5.40	38	7.09
LJS*	(1)	1.2053	0.257	5.40	37	6.97 ($a=1.003$)
	(2)	1.2214	0.257	5.28	38	7.35 ($a=1.006$)
	(3)	1.2251	0.255	2.08	125	60.2 ($a=1.670$)
	(4)	1.2339	0.257	5.29	38	7.33 ($a=1.003$)
	(5)	1.1963	0.256	5.40	38	7.09 ($a=1.001$)

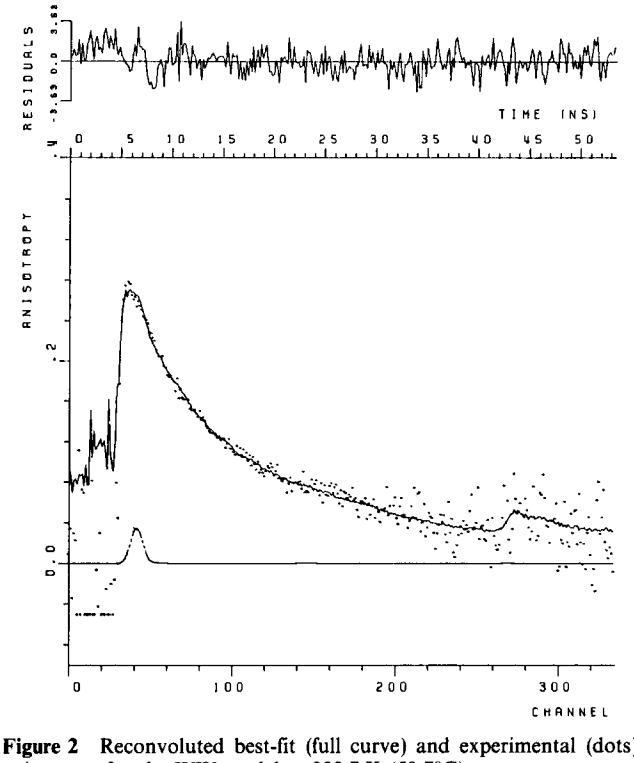

Figure 2 Reconvoluted best-fit (full curve) and experimental (dots) anisotropy for the WW model at 332.7 K (59.7°C)

The empirical formula suggested by Williams and Watts[18] leads to stable and consistent results. This fitting has been successfully used in dielectric relaxation[18] and light scattering whereas it yields an instability of parameters for polystyrene and polybutadiene studied by fluorescence anisotropy decay[5,6]. Because of its phe-

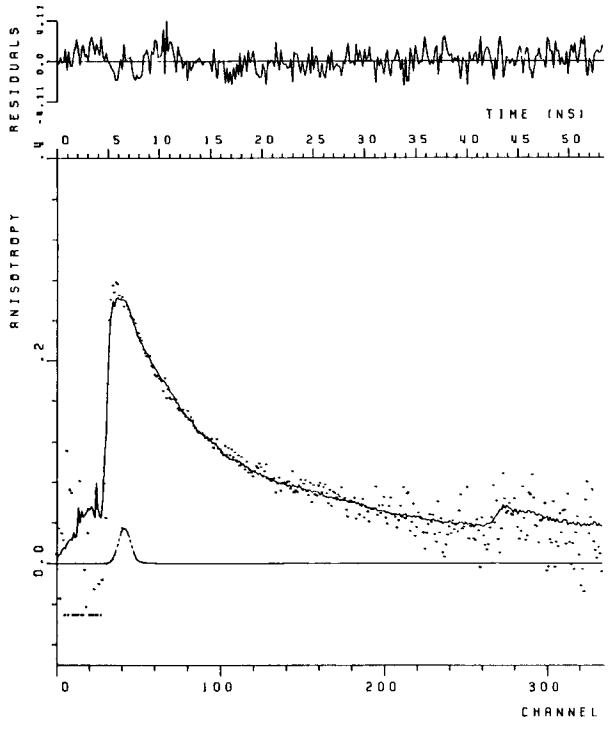

Figure 3 Reconvoluted best-fit (full curve) and experimental (dots) anisotropy for the BY model at 332.7 K (59.7°C)

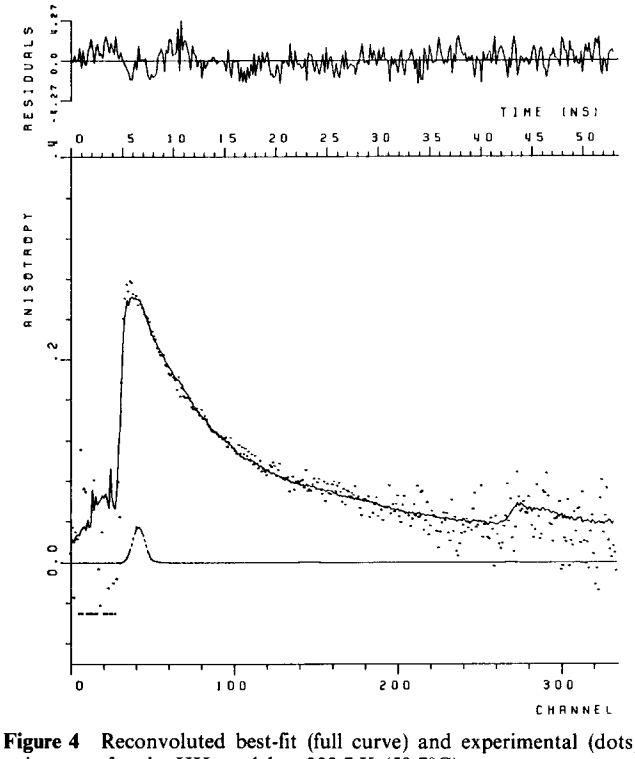

Figure 4 Reconvoluted best-fit (full curve) and experimental (dots) anisotropy for the HH model at 332.7 K (59.7°C)

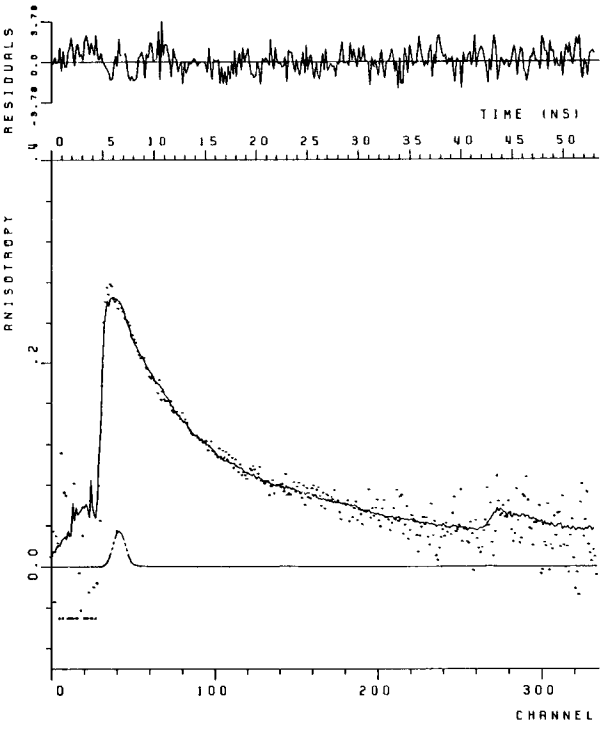

Figure 5 Reconvoluted best-fit (full curve) and experimental (dots) anisotropy for the GDL model at 332.7 K (59.7°C)

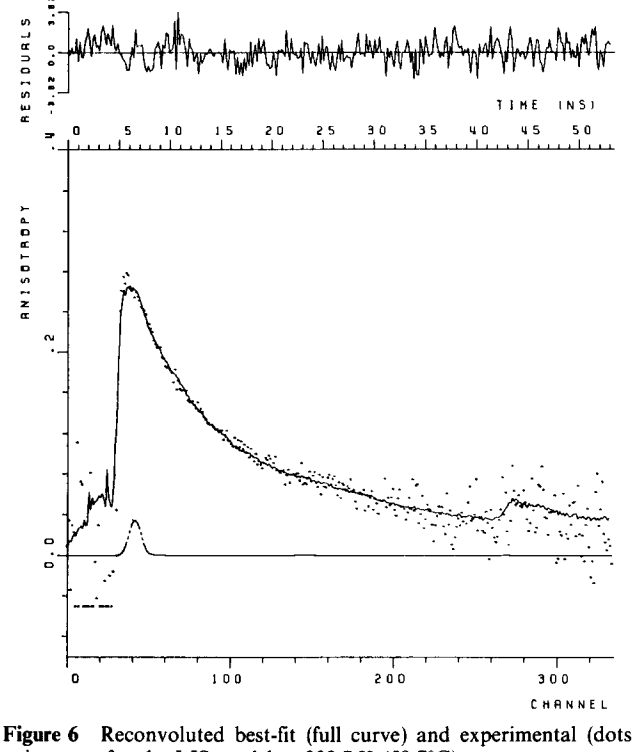

Figure 6 Reconvoluted best-fit (full curve) and experimental (dots) anisotropy for the LJS model at 332.7 K (59.7°C)

nomenological nature, this model does not provide much insight into the molecular dynamics, and we focused the following discussions on models based on a molecular description of chains.

The molecular models of Valeur *et al.*[1], on the one hand, and of Jones and Stockmayer[3], on the other, do not lead to satisfactory results. Similar results have been obtained in the case of polybutadiene and they have been extensively discussed in previous work[6].

The Bendler–Yaris[4] (BY), Hall–Helfand[7] (HH), generalized diffusion and loss[5] (GDL) and Lin–Jones–Stockmayer[9] (LJS) models lead to rather close values of χ^2 and they provide a stable fit to the OACF of PIAPI in IR307. The lowest values of χ^2 are obtained with the BY model, closely followed by GDL and LJS models. The BY model is difficult to interpret since it involves arbitrary truncations and thus it is not used in the following section. It is worth noting that, among the

Table 6 Best-fit parameters for the WW, VJGM and BY models at $T=364.6$ K (91.6°C) in melt PI

Model	Truncation	χ^2	r_0	τ_1 (ns)	τ_2 (ns)	τ_2/τ_1 (or β)
WW	(1)	1.0843	0.25362	3.59		$\beta=0.607$
	(2)	0.99561	0.25410	3.58		$\beta=0.605$
	(3)	1.0312	0.24917	3.70		$\beta=0.634$
	(4)	1.0028	0.25416	3.58		$\beta=0.605$
	(5)	0.98911	0.25088	3.67		$\beta=0.614$
VJGM	(1)	1.1359	0.26695	4.99	12.2	2.44
	(2)	1.0694	0.26781	4.86	12.3	2.54
	(3)	1.0807	0.26021	6.50	10.5	1.61
	(4)	1.0800	0.26790	4.85	12.4	2.55
	(5)	1.0839	0.26611	5.04	12.2	2.43
BY	(1)	1.0987	0.22490	1.24	35.0	28.1
	(2)	1.0049	0.22509	1.23	35.8	28.9
	(3)	1.1045	0.22624	1.17	41.3	35.1
	(4)	1.0158	0.22517	1.23	35.9	29.1
	(5)	0.93822	0.22233	1.29	34.3	26.6

Table 7 Best-fit parameters for the JS model at $T=364.6$ K (91.6°C) in melt PI

Model	Truncation	χ^2	r_0	τ_1 (ns)
JS_1 (one bond)	(1)	2.7900	0.21439	5.06
	(2)	3.2812	0.21423	5.07
	(3)	4.8267	0.21863	4.77
	(4)	3.4333	0.21441	5.06
	(5)	3.2984	0.21161	5.15
JS_3 (five bonds)	(1)	1.1886	0.24033	4.71
	(2)	1.1429	0.24029	4.71
	(3)	1.1122	0.24388	4.52
	(4)	1.1623	0.24031	4.71
	(5)	1.0998	0.23824	4.77
JS_4 (seven bonds)	(1)	1.4998	0.27293	3.07
	(2)	1.5492	0.27270	3.08
	(3)	2.3457	0.26499	3.34
	(4)	1.5939	0.27275	3.08
	(5)	1.6368	0.27193	3.10
JS_5 (nine bonds)	(1)	2.3048	0.29473	2.44
	(2)	2.6056	0.29375	2.46
	(3)	3.3518	0.26289	3.36
	(4)	2.7160	0.29377	2.46
	(5)	2.8369	0.29526	2.43

Table 8 Best-fit parameters for the HH, GDL and LJS models at $T=364.6$ K (91.6°C) in melt PI

Model	Truncation	χ^2	r_0	τ_1 (ns)	τ_2 (ns)	τ_2/τ_1
HH	(1)	1.1111	0.223	3.71	25	6.81
	(2)	1.0224	0.223	3.68	25	7.00
	(3)	1.1134	0.225	3.45	31	9.16
	(4)	1.0343	0.223	3.68	25	7.00
	(5)	0.94868	0.221	3.82	25	6.55
GDL	(1)	1.0884	0.230	1.56	17	11.1
	(2)	0.99163	0.230	1.54	17	11.4
	(3)	1.0753	0.229	1.58	16	10.7
	(4)	1.0017	0.230	1.54	17	11.3
	(5)	0.94300	0.227	1.63	17	10.5
LJS*	(1)	1.0817	0.229	2.03	17	8.73 ($a=0.734$)
	(2)	0.99037	0.229	1.92	17	9.23 ($a=0.782$)
	(3)	1.0753	0.229	1.60	16	10.6 ($a=0.989$)
	(4)	1.0003	0.229	2.00	17	8.94 ($a=0.742$)
	(5)	0.93252	0.223	1.98	12	6.62 ($a=0.372$)

models relying upon a conformational basis, the HH expression yields the worst χ^2.

The evolution of best-fit parameters in the temperature range 295–365 K for HH and GDL models is given in *Table 9*. Considering the poor accuracy of correlation time τ_2, the evolution of this parameter as a function of temperature cannot be studied in detail. Nevertheless, it is noteworthy that the ratio τ_2/τ_1 does not seem to vary significantly with temperature. The decrease of correlative pair transition time τ_1 is plotted as a function of $10^3/(T-T_\infty)$ in *Figure 7*. T_∞ denotes the Vogel temperature. This graphical representation derives from the WLF equation[14]:

$$\log\frac{\tau(T)}{\tau(T_0)}=-\frac{C_1^0(T-T_0)}{C_2^0+(T-T_0)} \tag{6}$$

where C_1^0 and C_2^0 are the WLF parameters at the temperature T_0. Expression (6) may be also written as:

$$\log\frac{\tau(T)}{\tau(T_0)}=-C_1^0+C_1^0C_2^0\frac{T}{T-T_\infty} \tag{7}$$

where $T=T_0-C_2^0$, and T_∞ and $C_1^0C_2^0$ are independent of

Table 9 Best-fit parameters for melt PI at different temperatures

T (°C)	Model	χ^2	r_0	τ_1 (ns)	τ_2 (ns)	τ_2/τ_1
21.9	HH	5.4	0.273	157	(2449)	15.6
	GDL	5.4	0.274	73.4	(1750)	23.9
32.5	HH	2.1	0.258	53.1	89.7	1.69
	GDL	2.2	0.258	32.7	66.2	2.02
40.4	HH	1.6	0.254	30.1	81.9	2.72
	GDL	1.7	0.255	17.1	56.0	3.27
49.0	HH	1.9	0.266	14.1	159	11.3
	GDL	2.0	0.270	6.69	73.5	11.0
59.7	HH	1.3	0.254	11.0	59.6	5.42
	GDL	1.2	0.257	5.42	37.7	6.95
69.5	HH	1.7	0.264	6.35	53.6	8.45
	GDL	1.4	0.271	2.72	33.1	12.2
78.8	HH	1.5	0.261	4.62	37.8	8.18
	GDL	1.3	0.271	1.89	24.6	13.0
83.0	HH	1.05	(0.184)	3.31	17.0	5.14
	GDL	1.04	(0.188)	1.45	12.4	8.58
91.6	HH	1.11	0.223	3.71	25.3	6.81
	GDL	1.08	0.229	1.56	17.3	11.1

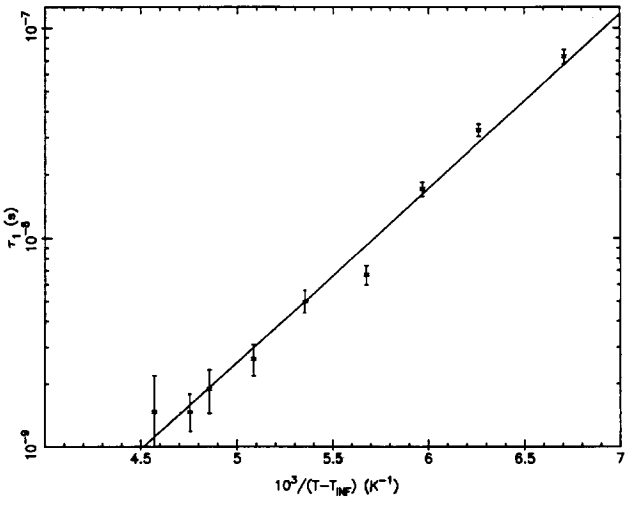

Figure 7 WLF plot of the best-fit relaxation time τ_1 (GDL model)

the reference temperature T_0. For practical reasons T_0 will be chosen equal to the glass transition temperature T_g. According to Ferry[15] the values of the WLF coefficients of natural rubber (all-*cis* polyisoprene) are the following:

$$C_1^g = 16.8$$

$$C_2^g = 58.6 \text{ K}$$

$$C_1^g C_2^g = C_1^0 C_2^0 \approx 900 \text{ K}$$

The slope of the curves obtained with the HH and GDL models are 813 K and 874 K, respectively. Hall and Helfand's model leads to a smaller C_1C_2 product than the theoretical value. In contrast, the data derived from the GDL expression fit the WLF relation rather well within experimental errors. This is a second argument suggesting that the dynamics of bulk polymers are described by the generalized diffusion and loss model better than by Hall and Helfand's model. The value of $\log \tau(T_g)$ may be found from the intercept of the straight line:

$$\log \tau(T_g) - C_1^g = -13$$

which yields:

$$\log \tau(T_g) \approx 3.6$$

The fact that the WLF equation accounts for the behaviour of τ_1 as a function of the temperature makes us think that the motions related to the correlation times τ_1 are involved in the glass transition process.

Our experiments corroborate the study of Viovy *et al.*[6] on labelled polybutadiene in bulk. In both cases, a very good fit is obtained using the GDL model, but the HH model also fits the data reasonably well. The temperature variation of correlation times is close to the macroscopic behaviour, as reflected in the WLF parameters. Finally, the ratio τ_2/τ_1 seems independent of temperature within experimental error for both polymers. It is worth noting, however, that the value of this ratio differs from one polymer to another. We obtain here 7 ± 2 and 10 ± 2 for HH and GDL models, respectively, whereas the values for PB[6] were 30 ± 10 and 30 ± 5. In spite of the relatively poor accuracy, these differences seem significant. We do not know, however, if this is an effect of the side-group in polyisoprene, or of the difference in microstructure between the two polymers studied.

STUDY OF LABELLED POLYISOPRENE IN DECALIN SOLUTION

The best-fit results for PIAPI in decalin are gathered in *Table 10*. As expected, the motions are much faster than in the bulk (lower τ_1). Because the pulse width of the excitation source is about 1 ns, this makes deconvolution more critical, and reduces the accuracy. Also, the truncation procedure used in the previous section becomes rather unpractical, since most of the information on the dynamics is already gathered in a narrow section of the experimental window (an example is given in *Table 10* for the HH model, showing that the stability of the parameters is however satisfactory).

In decalin, the LJS expression provides unstable parameters in solution (the best-fit values of a depend on the initial value in the reconvolution). This effect of the finite accuracy of computations reflects a very flat minimum of the χ^2 hypersurface, and it goes together with a wide confidence interval for the parameter. We previously concluded[10] that it is difficult to fit more than three independent parameters in a FAD experiment, because of the rapid increase of random noise in the 'tail' of the anisotropy. This is particularly true with the fast-decaying OACF encountered in fluid solutions.

More interestingly, one observes that the square residual of the HH model is lower than that of the GDL model, and corresponds to a very satisfactory fit. Indeed, our results are consistent with the main conclusions of previous work of Hyde *et al.* on polyisoprene in solution in hexane and cyclohexane using the picosecond holographic grating method[16]:

(a) The correlation time τ_1 is larger in decalin than in hexane or cyclohexane, which have smaller viscosities. This is in agreement with the idea that the timescale of the motions depends mainly on the viscosity of the solvent. The ratio of the relaxation times τ_1 in decalin and hexane equals ~ 5.8, whereas the viscosity ratio is ~ 8.0 at ~ 293 K, but this may be an effect of different microstructures.

(b) The ratio τ_2/τ_1 does not vary with the nature of the solvent within experimental errors: the value obtained by Hyde *et al.* is 3.6 ± 0.5, and our experiment leads to 4.3 ± 0.8. This supports the idea that, in a molecular solvent, τ_2/τ_1 may be considered as a characteristic parameter of the polymer chain, although this conclusion should still be considered with care. On the one hand Hyde's polymer and ours differ in their microstructure, which may fortuitously compensate for solvent effects. On the other hand, the two solvents used in ref. 16 are chemically very similar, and it is possible that more dissimilar solvents would affect τ_1/τ_2 significantly (see also ref. 17).

Table 10 Best-fit parameters for PI in decalin solution at $T = 298.2$ K (25.2°C)

Model	Truncation	χ^2	r_0	τ_1 (ns)	τ_2 (ns)	τ_2/τ_1 (or β)
1 exp (JS_1 (one bond))	20/468	4.512	0.203	2.030		
HH	20/468	1.027	0.237	1.428		4.32
	15/390	0.999	0.237	1.427		4.34
GDL	20/468	1.052	0.252	0.514		9.86
LJS*	20/468	1.025	0.246	0.368		13.50 ($a = 1.45$)
VJGM	20/468	1.189	0.328	$\rho = 0.91$	$\theta = 4.431$	
WW	20/468	1.056	0.290	1.05		$\beta = 0.59$
BY	20/468	1.022	0.239	0.480	8.230	
JS_3 (five bonds)	20/468	1.684	0.256	1.56		
JS_4 (seven bonds)	20/468	1.683	0.331	0.801		
JS_5 (nine bonds)	20/468	2.243	0.418	0.473		

CONCLUSIONS

This detailed study of the orientational autocorrelation function of labelled polyisoprene in the bulk confirms the wide generality of the models for local dynamics based on one-dimensional diffusion of excitations along the chain (Hall–Helfand, Lin–Jones–Stockmayer, generalized diffusion and loss). In an attempt to be more selective, it is worth noticing that, using the same labelled chain and the same experimental technique in bulk and in solution, the best fit was provided by the GDL expression in the bulk (as in our previous experiments in bulk polybutadiene[6]), and by the HH expression in dilute solutions (as in the experiments of Hyde *et al.*[16]). Therefore, we believe that this difference between earlier results is not an artefact, and that it is physically significant. Dynamics in the bulk appear to involve higher-order Bessel functions. As indicated in ref. 5, this can be interpreted qualitatively as a mixing of self- and (intramolecular) cross-correlations of segments. Why this mixing should be favoured by a polymer environment is still to be understood, however.

Another difference between dynamics in the bulk and in solution lies in the value of the ratio τ_2/τ_1. We showed rather unambiguously that this ratio is higher in a bulk polymer, indicating that the conformational memory of the chain extends on a longer length scale than in a solvent of small molecules. Indeed it is reasonable that a solvent that has a short-ranged and fast-decaying pair correlation function rapidly dissipates the energy transmitted to it by backbone motions, which corresponds to a stronger 'damping' of excitations along the chain. However these arguments have not yet been put on a firm theoretical ground, like most problems dealing with intermolecular dynamic effects. In short, this set of experiments support the models based on conformational dynamics of an isolated chain as far as the shape of the correlation function is concerned, but they also point out the limits of such models when trying to correlate the dynamic parameters with the chain structure and environment.

ACKNOWLEDGEMENTS

We are indebted to La Manufacture de Pneumatiques Michelin for the synthesis of the labelled polyisoprene and to the CNRS 'Laboratoire pour l'Utilisation du Rayonnement Electromagnetique' (LURE) for allocation of synchrotron beam time. We are particularly grateful to Dr J. C. Brochon and Dr F. Merola for their assistance in the experiments at LURE.

REFERENCES

1 Valeur, B., Jarry, J. P., Gény, F. and Monnerie, L. *J. Polym. Sci., Polym. Phys. Edn.* 1975, **13**, 667
2 Valeur, B., Monnerie, L. and Jarry, J. P. *J. Polym. Sci., Polym. Phys. Edn.* 1975, **13**, 675
3 Jones, A. A. and Stockmayer, W. H. *J. Polym. Sci., Polym. Phys. Edn.* 1977, **15**, 847
4 Bendler, J. T. and Yaris, R. *Macromolecules* 1978, **11**, 650
5 Viovy, J. L., Monnerie, L. and Brochon, J. C. *Macromolecules* 1983, **16**, 1845
6 Viovy, J. L., Monnerie, L. and Merola, F. *Macromolecules* 1985, **18**, 1130
7 Hall, C. K. and Helfand, E. *J. Chem. Phys.* 1982, **77** (6), 3275
8 Weber, T. W. and Helfand, E. *J. Phys. Chem.* 1983, **87**, 2881
9 Lin, Y. Y., Jones, A. A. and Stockmayer, W. H. *J. Polym. Sci., Polym. Phys. Edn.* 1984, **22**, 2195
10 Viovy, J. L. and Monnerie, L. *Adv. Polym. Sci.* 1985, **67**, 100
11 Wahl, P. *Chem. Phys.* 1977, **22**, 245
12 Wahl, P. *Nato ASI Ser. (A): Life Sci.* 1980, **69**, 483
13 Veissier, V., Viovy, J. L. and Monnerie, L. Proc. Workshop on Polymer Motion in Dense Systems, Grenoble, 23–25 Sept. 1987 (Eds. D. Richter and T. Springer), Springer-Verlag, Berlin, 1988; *Springer Proc. Phys.* 1988, **28**, 37
14 Williams, M. L., Landel, R. F. and Ferry, J. D. *J. Am. Chem. Soc.* 1955, **77**, 3701
15 Ferry, J. D. 'Viscoelastic Properties of Polymers', Wiley, New York, 1970
16 Hyde, P. D., Waldow, D. A., Ediger, M. D., Kitano, T. and Ito, K. *Macromolecules* 1986, **19**, 2533
17 Viovy, J. L., Monnerie, L., Veissier, V. and Fofana, M. 'Applications of Lasers in Polymer Science and Technology' (Eds. J. P. Fouassier and J. F. Rabek), CRC Press, Boca Raton, FL, 1989
18 Williams, G. and Watts, D. C. *Trans. Faraday Soc.* 1970, **66**, 80